REMUNOM
ISSN 2178-6925

Received: 13/03/2026 - **Accepted:** 20/05/2026
Vol: 13.10
DOI: 10.66104/fn0sgw57
Pages: 1-27

PROJETO INTEGRADO E VERIFICAÇÃO NUMÉRICA DE SISTEMA DE FREIOS A DISCO PARA VEÍCULO OFF-ROAD LEVE UTILIZANDO ANÁLISE POR ELEMENTOS FINITOS

INTEGRATED DESIGN AND NUMERICAL VERIFICATION OF A DISC BRAKE SYSTEM FOR A LIGHT OFF-ROAD VEHICLE USING FINITE ELEMENT ANALYSIS

DISEÑO INTEGRADO Y VERIFICACIÓN NUMÉRICA DE UN SISTEMA DE FRENOS DE DISCO PARA UN VEHÍCULO TODOTERRENO LIGERO MEDIANTE ANÁLISIS DE ELEMENTOS FINITOS.

Geovani Santos Borges
Mestrando em Engenharia Mecânica, Universidade Federal da Paraíba (UFPB) – João Pessoa, Brasil
E-mail: geovani.santos.borges@gmail.com

Paulo Ricardo de Oliveira Queiroz
Mestre em Engenharia Mecânica, Instituto Federal de Educação, Ciência e Tecnologia da Paraíba (IFPB) – *campus* Cajazeiras, Brasil
E-mail: paulo.queiroz@ifpb.edu.br

Victor Wagner Rodrigues Batista
Graduando em Engenharia de Controle e Automação, Instituto Federal de Educação, Ciência e Tecnologia da Paraíba (IFPB) – *campus* Cajazeiras, Brasil
E-mail: victor.wagner@academico.ifpb.edu.br

Felipe Carvalho da Silva
Mestrando em Engenharia Mecânica, Universidade Federal da Paraíba (UFPB) – João Pessoa, Brasil
E-mail: felipecarvalho492001@gmail.com

Edleusom Saraiva da Silva
Mestre em Engenharia Mecânica, Instituto Federal de Educação, Ciência e Tecnologia da Paraíba (IFPB) – *campus* Cajazeiras, Brasil
E-mail: edleusom.silva@ifpb.edu.br

Rairton Helder Façanha Júnior
Especialista em Engenharia de Segurança do Trabalho, Instituto Federal de Educação, Ciência e Tecnologia da Paraíba (IFPB) – *campus* Cajazeiras, Brasil
E-mail: rairton.facanha@ifpb.edu.br

Leonardo Pereira de Lucena Silva
Mestre em Engenharia Mecânica, Instituto Federal de Educação, Ciência e Tecnologia da Paraíba (IFPB) – *campus* Cajazeiras, Brasil
E-mail: lucena.leonardo@ifpb.edu.br

REMUNOM
ISSN 2178-6925

Received: 13/03/2026 - **Accepted:** 20/05/2026
Vol: 13.10
DOI: 10.66104/fn0sgw57
Pages: 1-27

Luiz Paulo de Oliveira Queiroz
Doutor em desenvolvimento e meio ambiente, UFERSA, Mossoró, RN, Brasil,
E-mail: luiz.paulo@ifce.edu.br

Resumo

Sistemas de freios a disco aplicados a veículos off-road de pequeno porte estão sujeitos a severas solicitações termomecânicas, decorrentes de carregamentos dinâmicos variáveis, superfícies de baixa aderência e eventos de frenagem de curta duração e elevada energia. Embora a literatura aborde aspectos isolados, como análise estrutural, seleção de materiais e dimensionamento hidráulico, ainda são escassas abordagens que integrem, de forma coerente e verificável, a dinâmica veicular, o dimensionamento hidromecânico e a verificação computacional, especialmente em plataformas leves do tipo Baja SAE. Este trabalho propõe e verifica numericamente uma metodologia de projeto integrada, estruturada em cinco fases, para o desenvolvimento de um sistema de freios a disco para um protótipo Baja SAE. A abordagem combina modelagem analítica da dinâmica longitudinal, baseada em modelo de dois graus de liberdade, modelagem paramétrica em CAD e simulações por elementos finitos (FEA), incluindo análises estruturais e térmica transiente, com verificação por modelo de capacitância concentrada. Os resultados indicam que a frenagem a 0,60 g eleva a força normal no eixo dianteiro em 78,6%, concentrando 59,6% da força de frenagem, justificando a adoção de discos assimétricos. O sistema apresentou eficiência superior a 90% para $\mu = 0,60$, com tendência ao bloqueio traseiro para $\mu > 0,70$. As análises estruturais confirmaram regime elástico, com fatores de segurança de 2,46 para o pedal (SAE 1020) e superiores a 2,52 para os discos (SAE 1045). A simulação térmica indicou temperatura máxima de 237 °C na interface pastilha–disco ao final de 3 s, abaixo da faixa crítica de degradação (~300–400 °C), com boa concordância entre os modelos numérico e analítico. A metodologia proposta demonstra que a integração entre dinâmica veicular, dimensionamento analítico e simulação computacional constitui abordagem eficaz e reprodutível para o projeto de sistemas de frenagem em veículos off-road de pequeno porte.

Palavras-chave: freios; Baja; dinâmica; simulação; FEA.

Abstract

Disc brake systems applied to small off-road vehicles are subject to severe thermomechanical stresses resulting from variable dynamic loads, low-grip surfaces, and short-duration, high-energy braking events. Although the literature addresses isolated aspects such as structural analysis, material selection, and hydraulic design, approaches that coherently and verifiably integrate vehicle dynamics, hydromechanical design, and computational verification are still scarce, especially in lightweight platforms such as Baja SAE. This work proposes and numerically verifies an integrated design methodology, structured in five phases, for the development of a disc brake system for a Baja SAE prototype. The approach combines analytical modeling of longitudinal dynamics, based on a two-degree-of-freedom model, parametric modeling in CAD, and finite element analysis (FEA) simulations,

REMUNOM
ISSN 2178-6925

Received: 13/03/2026 - **Accepted:** 20/05/2026
Vol: 13.10
DOI: 10.66104/fn0sgw57
Pages: 1-27

including structural and transient thermal analyses, with verification by lumped capacitance modeling. The results indicate that braking at 0,60 g increases the normal force on the front axle by 78,6%, concentrating 59,6% of the braking force, justifying the adoption of asymmetrical discs. The system showed efficiency greater than 90% for μ = 0,60, with a tendency towards rear wheel lock-up for μ > 0,70. Structural analyses confirmed an elastic regime, with safety factors of 2,46 for the pedal (SAE 1020) and greater than 2,52 for the discs (SAE 1045). Thermal simulation indicated a maximum temperature of 237 °C at the pad-disc interface at the end of 3 s, below the critical degradation range (~300–400 °C), with good agreement between the numerical and analytical models. The proposed methodology demonstrates that the integration of vehicle dynamics, analytical design, and computational simulation constitutes an effective and reproducible approach for the design of braking systems in small off-road vehicles.

Keywords: brakes; Baja; dynamics; simulation; FEA.

Resumen

Los sistemas de frenos de disco aplicados a vehículos todoterreno pequeños están sujetos a severas tensiones termomecánicas derivadas de cargas dinámicas variables, superficies de baja adherencia y eventos de frenado de corta duración y alta energía. Si bien la literatura aborda aspectos aislados como el análisis estructural, la selección de materiales y el diseño hidráulico, aún son escasos los enfoques que integran de manera coherente y verificable la dinámica del vehículo, el diseño hidromecánico y la verificación computacional, especialmente en plataformas ligeras como Baja SAE. Este trabajo propone y verifica numéricamente una metodología de diseño integrada, estructurada en cinco fases, para el desarrollo de un sistema de frenos de disco para un prototipo Baja SAE. El enfoque combina el modelado analítico de la dinámica longitudinal, basado en un modelo de dos grados de libertad, el modelado paramétrico en CAD y simulaciones de análisis de elementos finitos (FEA), incluyendo análisis estructurales y térmicos transitorios, con verificación mediante modelado de capacitancia concentrada. Los resultados indican que frenar a 0,60 g aumenta la fuerza normal en el eje delantero en un 78,6 %, concentrando el 59,6 % de la fuerza de frenado, lo que justifica la adopción de discos asimétricos. El sistema mostró una eficiencia superior al 90 % para μ = 0,60, con una tendencia al bloqueo de la rueda trasera para μ > 0,70. Los análisis estructurales confirmaron un régimen elástico, con factores de seguridad de 2,46 para el pedal (SAE 1020) y superiores a 2,52 para los discos (SAE 1045). La simulación térmica indicó una temperatura máxima de 237 °C en la interfaz pastilla-disco al final de 3 s, por debajo del rango de degradación crítico (~300–400 °C), con una buena concordancia entre los modelos numéricos y analíticos. La metodología propuesta demuestra que la integración de la dinámica del vehículo, el diseño analítico y la simulación computacional constituye un enfoque eficaz y reproducible para el diseño de sistemas de frenado en vehículos todoterreno pequeños.

Palabras clave: Frenos; Baja; dinámica; simulación; FEA.

REMUNOM
ISSN 2178-6925

Received: 13/03/2026 - **Accepted:** 20/05/2026
Vol: 13.10
DOI: 10.66104/fn0sgw57
Pages: 1-27

1. Introduction

Disc brake systems are critical safety subsystems in motor vehicles, responsible for the controlled conversion of kinetic energy into thermal energy through tribological contact between the brake pad and disc. The efficiency of this process directly governs the stopping distance, directional stability during deceleration, and the thermomechanical integrity of the components under cyclic loading. In small off-road vehicles, such as Baja SAE prototypes, light utility vehicles, and experimental platforms, these demands are significantly amplified: uneven terrain, abrupt variations in normal load, mechanical impacts, and low tire-to-ground adhesion coefficients impose more severe stresses on the braking system compared to those observed in conventional passenger vehicles. In the context of the Baja SAE competition, the official regulations establish minimum safety requirements for braking systems, demanding simultaneous locking of all four wheels and efficient actuation by drivers of different physical profiles (SAE BRASIL, 2024). These normative criteria define the design space and impose functional restrictions that must be met before vehicle homologation.

The design of hydraulic disc brake systems for this class of vehicle involves the interaction of multiple coupled physical phenomena, including tribological contact at the pad-disc interface, hydraulic pressure transmission, heat generation and dissipation by friction, and stress and strain fields in the structural components. In this context, the dynamic load transfer between axles during deceleration is a critical design variable, as it redistributes the normal forces on the tires as a function of longitudinal deceleration, center of gravity height, and wheelbase. In vehicles with a predominantly rear mass distribution, characteristic of Baja SAE prototypes, this phenomenon intensifies the braking demand on the front axle and increases the risk of premature locking of the rear wheels.

Finite element analysis (FEA) has become an essential tool in the development of braking systems, allowing for the integrated assessment of structural integrity and transient thermal behavior of components before the fabrication of physical prototypes. Recent studies demonstrate that thermomechanical approaches using FEA are

REMUNOM
ISSN 2178-6925

Received: 13/03/2026 - **Accepted:** 20/05/2026
Vol: 13.10
DOI: 10.66104/fn0sgw57
Pages: 1-27

capable of predicting, with high precision, temperature, stress, and strain fields in brake components under different loading conditions (Belhocine; Abdullah, 2020; Noohi et al., 2024; Oladeji et al., 2022).

Therefore, this work aims to develop and numerically verify a hydraulic disc brake system for a Baja SAE prototype, using an integrated methodology in five phases: (i) longitudinal dynamics and load transfer; (ii) hydromechanical design; (iii) parametric modeling in CAD; (iv) structural analysis by FEA; and (v) transient thermal simulation with verification by lumped capacitance model. This study is positioned as a preliminary numerical and analytical verification, not as an experimental validation of a final system.

2. Literature Review

2.1. Hydraulic Braking Principles

Hydraulic brake systems operate by amplifying and transmitting forces through incompressible fluid, according to Pascal's principle. The relationship between the force applied by the driver on the pedal, the geometry of the lever system, and the effective areas of the master cylinder and caliper pistons determines the compression force exerted on the discs, directly governing the braking torque generated at each wheel (Budynas; Nisbett, 2020). The system's performance is a function of the tribological friction coefficient between the pad and the disc, the hydraulic pressure generated, and the geometric characteristics of the components, variables that interact in a coupled manner and whose combined effects must be verified analytically and by numerical simulation (Belhocine; Abdullah, 2020).

The frictional contact between the brake pad and the disc is the central phenomenon of the braking process: the vehicle's kinetic energy is converted into thermal energy, imposing transient temperature gradients on the disc that induce thermomechanical stresses superimposed on the mechanical stresses of the contact pressure. Noohi et al. (2024) demonstrated, through experimental modal analysis and FEA, that the contact stiffness at the pad-disc interface exhibits a non-linear

REMUNOM
ISSN 2178-6925

Received: 13/03/2026 - **Accepted:** 20/05/2026
Vol: 13.10
DOI: 10.66104/fn0sgw57
Pages: 1-27

dependence on braking pressure, highlighting the complexity of the system's dynamic behavior.

2.2. Dynamic Load Transfer and Braking Force Distribution

During deceleration, the inertial force applied at the center of gravity generates a moment that redistributes the normal reactions between the axles, characterizing the dynamic load transfer (DLT). This effect depends on the vehicle's deceleration normalized by gravity (a/g), the height of the center of gravity (CG) (H), and the wheelbase (L), according to the longitudinal two-degree-of-freedom model (El-Gindy; El-Sayegh, 2023), and can transfer a significant portion of the load to the front axle (Savio et al., 2022).

The ideal braking distribution is defined by the parabolic curve that maximizes the use of grip without premature locking. Efficiency (η) measures the proximity between the actual distribution and this ideal condition. In light off-road vehicles, stability at low coefficients of friction is prioritized, which implies underutilization of the rear axle at high grip as an inherent limitation of fixed-ratio systems (El-Gindy; El-Sayegh, 2023).

2.3. Structural FEA of Brake Components

Structural analysis using FEA has become the standard approach for verifying the mechanical integrity of brake system components, allowing the identification of stress concentration regions, evaluating the safety factor in relation to the yield strength using the von Mises criterion, and guiding design decisions before manufacturing (Budynas; Nisbett, 2020). Reghunath et al. (2021) performed structural and thermal analyses of a disc-caliper assembly for a competition vehicle using ANSYS Workbench, confirming the method's ability to predict critical failure regions with accuracy comparable to experimental results. Prakash and Prakash (2024) extended this approach to the comparative analysis of alternative materials for brake discs, demonstrating that medium-carbon steel, such as SAE 1045, exhibits

REMUNOM
ISSN 2178-6925

Received: 13/03/2026 - **Accepted:** 20/05/2026
Vol: 13.10
DOI: 10.66104/fn0sgw57
Pages: 1-27

satisfactory thermomechanical performance compared to lighter composites when considering structural strength, thermal conductivity, and wear resistance together.

2.4. Transient Thermal Behaviour of Brake Discs

Thermal management of brake discs is critical for system reliability, as increased temperature can induce thermal fade and reduce braking efficiency (Yin et al., 2023). Transient thermal analysis using FEA allows for the estimation of the temperature field evolution, considering heat generated by friction and convection as the main dissipation mechanism (Belhocine; Abdullah, 2020). Studies indicate that solid carbon steel discs reach temperatures of approximately 200–240 °C during short-duration braking events (Oladeji et al., 2022). The incorporation of ventilation holes reduces mass and increases the heat exchange area, accelerating cooling and mitigating the risk of fade (Chaturvedi et al., 2023). As a verification, the lumped capacitance model provides consistent estimates of cooling time in natural convection regimes (Yin et al., 2023).

3. Methodology

The system was developed through an iterative integrated methodology structured in five sequential phases with defined acceptance criteria. It articulates analytical vehicle-dynamics methods, parametric CAD, and FEA, ensuring traceability before physical implementation. The model represents a simplified longitudinal braking condition on a flat, homogeneous surface, not the full off-road operating spectrum, which must be considered when interpreting the results

3.1. Phase I – Literature Review

Searches conducted in Scopus, Web of Science, and Google Scholar data-bases, covering the period from 2018 to 2025, resulted in the selection of 14 references directly aligned with the theoretical and methodological framework of this study. These

REMUNOM
ISSN 2178-6925

Received: 13/03/2026 - **Accepted:** 20/05/2026
Vol: 13.10
DOI: 10.66104/fn0sgw57
Pages: 1-27

works were critically analyzed to ensure consistency with current approaches in the field and to support the adopted modeling and design procedures. Based on this review, the minimum functional requirements of the system were established and are summarized in Table 1.

Table 1: Minimum functional requirements established for the braking system.

Requirement	Acceptance Criterion	Basis
Simultaneous wheel lock	All four wheels locked simultaneously	SAE Brasil (2024)
Maximum pedal effort	≤ 500 N (female drivers)	Budynas; Nisbett (2020)
Maximum disc temperature	< Fade limit — SAE 1045 (~300–400 °C)	Yin et al. (2023)
Structural safety factor	FS ≥ 1,5 (pedal); FS ≥ 2,0 (discs)	Budynas; Nisbett (2020)
Braking efficiency	η > 80% for μs = 0,60	Savio et al. (2022)

Source: Authors, 2026.

3.2. Phase II – Vehicle Parameters

Parameters were obtained from literature on similar off-road platforms (El-Gindy; El-Sayegh, 2023; Reghunath et al., 2021). The CG longitudinal position yields a static distribution of 33,3% front / 66,7% rear. The tyre–ground friction coefficient (μs = 0,60) was based on experimental data for compacted irregular surfaces (Savio et al., 2022). All parameters are consolidated in Table 2.

Table 2: Geometric and dynamic parameters adopted for sizing.

Parameter	Symbol	Value	Source
Total mass (driver included)	*m*	260 kg	El-Gindy; El-Sayegh (2023)
Wheelbase	*L*	1,50 m	Estimated
CG–rear axle distance	*c*	0,50 m	Estimated
CG–front axle distance	*b*	1,00 m	Estimated
Centre-of-gravity height	*H*	0,65 m	Estimated
Maximum operating speed	*Vmax*	11,1 m/s	Estimated
Tyre–ground friction coeff.	*μs*	0,60	Savio et al. (2022)
Pad–disc friction coeff.	*μp*	0,50	Reghunath et al. (2021)

REMUNOM
ISSN 2178-6925

Received: 13/03/2026 - **Accepted:** 20/05/2026
Vol: 13.10
DOI: 10.66104/fn0sgw57
Pages: 1-27

Calliper piston diameter	*Dp*	34 mm	Commercial
Master cylinder bore	*Dc*	19,5 mm	Commercial
Pedal mechanical advantage	*R*	6 : 1	Budynas; Nisbett (2020)
Effective tyre radius	*Rp*	0,279 m	Tyre 23×7–10 in
Front disc diameter	*Dd,f*	160 mm	Phase III design
Rear disc diameter	*Dd,r*	140 mm	Phase III design

Source: Authors, 2026.

3.3. Phase III – Analytical Sizing

The sizing follows the logical chain in Table 3, which presents all ten governing equations with descriptions of variables. Table 3 also serves as a verification matrix: cross-checking input parameters against Table 2 confirms that no undeclared variables are introduced, ensuring reproducibility.

Table 3: Analytical sizing — governing equations, formulas, and variable descriptions.

Eq.	Formula	Description of variables
(1)	$Fet = W \cdot b / L \quad and \quad Fed = W \cdot c / L$	Static normal reactions: Fet (rear), Fed (front); W = total weight; b, c = CG–axle distances; L = wheelbase
(2)	$Fn,f = Fed + W \cdot (a/g) \cdot (H/L) \quad and$ $Fn,r = Fet - W \cdot (a/g) \cdot (H/L)$	Dynamic load transfer; a = deceleration; g = 9.81 m/s²; H = CG height
(3)	$Ff = Fn \cdot \mu s$	Maximum braking force per axle; μs = tyre–ground friction coefficient
(4)	$Tn = Ff \cdot Rp$	Required braking torque per wheel; Rp = effective tyre radius
(5)	$Fat = 2 \cdot Tn / Dd$	Pad friction force on disc; Dd = disc diameter
(6)	$Fn = Fat / \mu p$	Disc normal force; μp = pad–disc friction coefficient
(7)	$P = Fn / Ap$	Hydraulic pressure; Ap = calliper piston area = π(Dp/2)²
(8)	$Fhc = Fn \cdot (Dc / Dp)^2$	Master cylinder rod force; Dc = master cylinder bore; Dp = piston diameter
(9)	$Fpedal = Fhc / R$	Pedal effort; R = mechanical advantage (lever ratio)
(10)	$d = v_0^2 / (2 \cdot a)$	Stopping distance; v_0 = initial speed; a = deceleration

Source: Authors, 2026

REMUNOM
ISSN 2178-6925

Received: 13/03/2026 - **Accepted:** 20/05/2026
Vol: 13.10
DOI: 10.66104/fn0sgw57
Pages: 1-27

3.3.1. Static equilibrium and dynamic load transfer

Normal reactions on rear (Fet) and front (Fed) axles are first determined from static equilibrium (Eq. 1). Load distribution depends exclusively on CG position. During braking, longitudinal deceleration generates inertial force at the CG, producing load transfer to the front axle described by the two-degree-of-freedom longitudinal model (Eq. 2) (El-Gindy; El-Sayegh, 2023).

3.3.2. Braking forces and torques

The maximum braking force at each axle is limited by tyre–ground grip (Eq. 3), and required wheel torque is obtained by multiplying by the effective tyre radius (Eq. 4).

3.3.3. Disc–pad assembly and hydraulic system

The chain from Eq. 5 to Eq. 10 converts required torque into pad friction force (Eq. 5), disc normal force (Eq. 6), hydraulic pressure (Eq. 7), master cylinder rod force (Eq. 8), pedal effort (Eq. 9), and stopping distance (Eq. 10). Hydraulic pressure P = 1,75 MPa corresponds to one front calliper piston ($Ap = \pi \cdot (0{,}034/2)^2$ m²).

3.4. Phase IV – Parametric CAD Model

Pedal, front disc (Ø160 mm), and rear disc (Ø140 mm) were modelled in a parametric 3D CAD environment, enabling automatic geometry updates. Discs were designed with ventilation holes to reduce mass and increase heat-exchange area (Chaturvedi et al., 2023; Oladeji et al., 2022). Simulations were conducted in ANSYS Workbench 2024, encompassing static structural and transient thermal analyses conducted independently (not thermally–structurally coupled), preceded by a mesh convergence study.

REMUNOM
ISSN 2178-6925

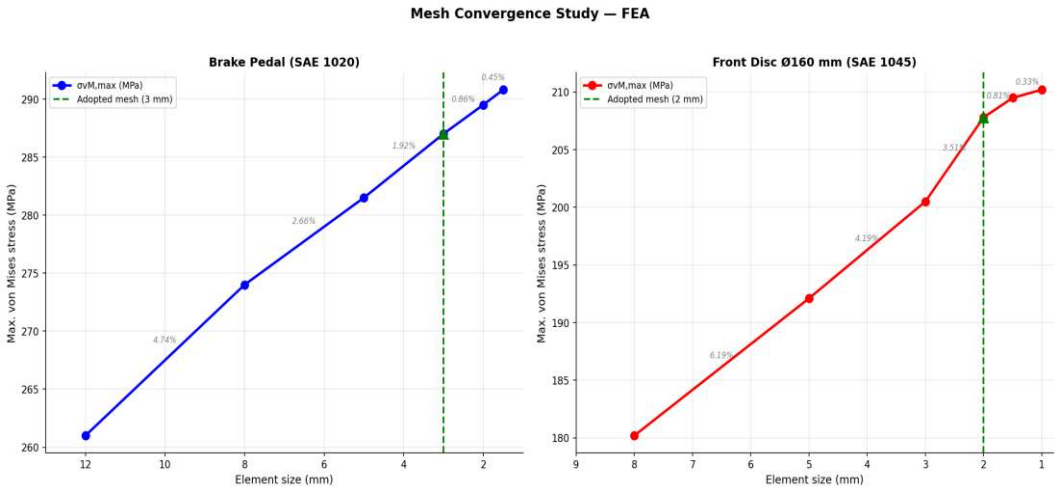
Received: 13/03/2026 - **Accepted:** 20/05/2026
Vol: 13.10
DOI: 10.66104/fn0sgw57
Pages: 1-27

3.5. Phase V – Finite Element Simulations (FEA)

3.5.1. Mesh convergence study

Progressive mesh refinement was applied, halving element size at each step, monitoring maximum von Mises stress (pedal) and maximum nodal temperature (disc). A variation criterion of less than 2% between consecutive refinements was adopted (Noohi et al., 2024). Figure 1 shows asymptotic convergence for both quantities. The final discretisation was set at 3 mm for the pedal and 2 mm for the disc.

Figure 1. Mesh convergence study — FEA: maximum von Mises stress vs. element size for the brake pedal (left) and front disc (right).



Source: Authors, 2026

3.5.2. Static structural analysis

Mechanical integrity was verified using the von Mises yield criterion (FS = Sy / σvM,max). SAE 1020 was adopted for the pedal (Sy = 350 MPa) and SAE 1045 for the discs (Sy = 530 MPa), with properties from Gerdau (2020). Boundary conditions and loads are described in Table 4. The load of 6.384 N on the discs is an intentionally oversized condition as a conservative structural verification strategy. The final meshes comprised approximately 28.500 nodes and 17.800 elements for the pedal, and 41.200 nodes and 26.500 elements for each disc. Mesh quality metrics (average skewness < 0,25; average aspect ratio < 3,0) confirmed adequate element regularity for the adopted element type.

REMUNOM
ISSN 2178-6925

Received: 13/03/2026 - **Accepted:** 20/05/2026
Vol: 13.10
DOI: 10.66104/fn0sgw57
Pages: 1-27

Table 4: Parameters of the static structural FEA simulations.

Component	Material	Sy (MPa)	Load (N)	Restraint	Element	Size
Brake pedal	SAE 1020	350	523,72	Fixed at chassis pivot	Quadratic tetrahedral	3 mm
Front disc	SAE 1045	530	6.384*	Fixed at hub	Quadratic tetrahedral	2 mm
Rear disc	SAE 1045	530	6.384*	Fixed at hub	Quadratic tetrahedral	2 mm

*Conservative oversized condition for structural verification.
Source: Authors, 2026.

3.5.3. Transient thermal analysis and lumped-capacitance model

Heat flux at the pad–disc interface was estimated as the product of μp, normal force, and tangential velocity, distributed over the effective contact area. The effective contact area was computed as the annular pad footprint on the disc, corresponding to approximately 1.850 mm² for the front disc and 1.420 mm² for the rear disc, consistent with the caliper geometry adopted (Belhocine; Abdullah, 2020). Lumped-capacitance verification was applied using $T(t) = Tamb + (T_0 - Tamb)\cdot\exp(-t/\tau)$, with $\tau = \rho\cdot V\cdot cp/(h\cdot A)$, applicable when $Bi < 0,1$ (Yin et al., 2023). Parameters are presented in Table 5.

Table 5: Parameters of the transient thermal FEA analysis.

Parameter	Value	Source
Initial temperature	23 °C	—
Braking event duration	3 s	Oladeji et al. (2022)
Convection coefficient h	80 W/m²K	Yin et al. (2023)
Thermal conductivity k – SAE 1045	51,9 W/m·K	Gerdau (2020)
Specific heat cp – SAE 1045	477 J/kg·K	Gerdau (2020)
Thermal operating limit – SAE 1045	~600 °C	Ashby; Jones (2012)
Element type	Quadratic tetrahedral	—
Element size	2 mm	Section 3.5.1 convergence

Source: Authors, 2026.

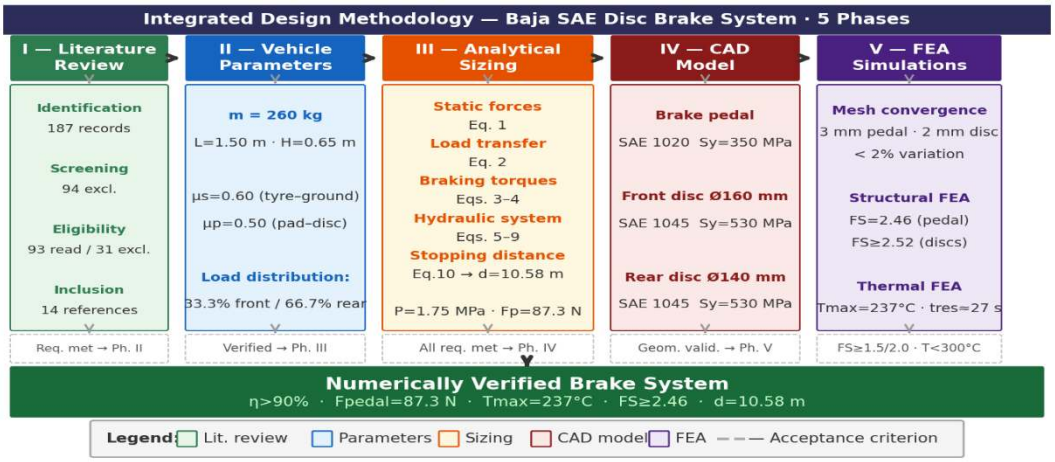
REMUNOM
ISSN 2178-6925

Received: 13/03/2026 - **Accepted:** 20/05/2026
Vol: 13.10
DOI: 10.66104/fn0sgw57
Pages: 1-27

3.6. Methodology Summary

Figure 2 summarises the integrated design methodology in five sequential, iterative phases, demonstrating the traceability between analytical sizing and numerical FEA verification, with phase progression conditioned on the results obtained at each step. The methodology was applied in its entirety to the brake system development, from initial parameter definition to the integrated structural and thermal computational verification that verifies the functional requirements established in Table 1.

Figure 1: Flowchart of the iterative integrated design methodology, structured in five sequential phases.



Source: Authors, 2026.

4. Results and Discussion

This section presents and discusses the results of the integrated brake system design, encompassing everything from analytical dimensioning to structural and thermal verification using FEA. The results are compared with recent literature, with the aim of numerically verifying the adopted models and demonstrating the consistency of the proposed approach.

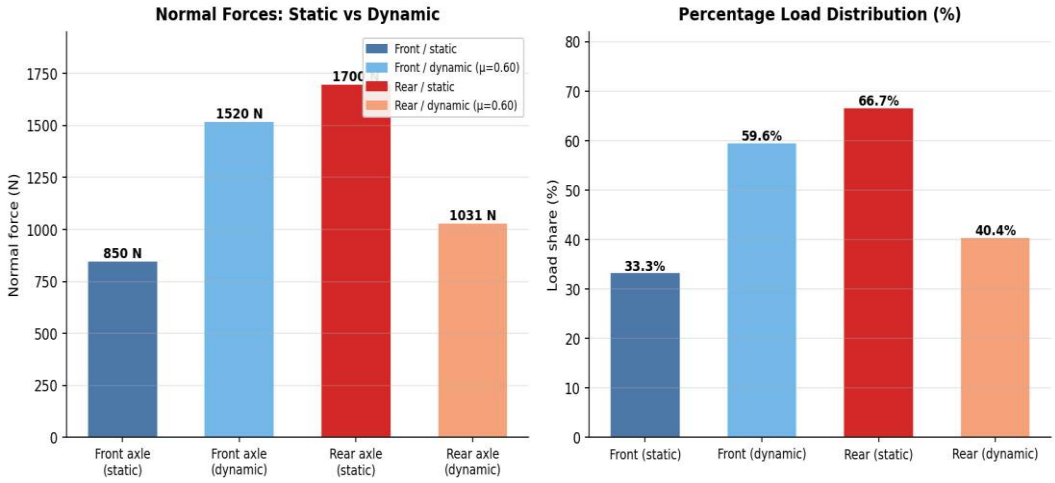
4.1. Analytical Dimensioning of the Brake System

REMUNOM
ISSN 2178-6925

Received: 13/03/2026 - **Accepted:** 20/05/2026
Vol: 13.10
DOI: 10.66104/fn0sgw57
Pages: 1-27

The results of the analytical dimensioning of the brake system are presented in Figures 3 and 4. The static normal forces on the rear axle (Fet = 1.700 N) and front axle (Fed = 850,2 N) reflect the adopted load distribution (66,7%/33,3%). During braking at μ = 0,60, the dynamic load transfer increases the normal force on the front axle to 1.519,61 N, which corresponds to an increase of 78,6% compared to the static condition, while on the rear axle, there is a reduction to 1.030,99 N (−39,4%). This behavior is in agreement with the literature (Savio et al., 2022; Tung; Van Van, 2023) and shows the load migration to the front axle, with a direct impact on the distribution of braking forces, as illustrated in Figure 3.

Figure 2: Static and dynamic normal forces per axle and percentage load distribution during braking (μ = 0,60).



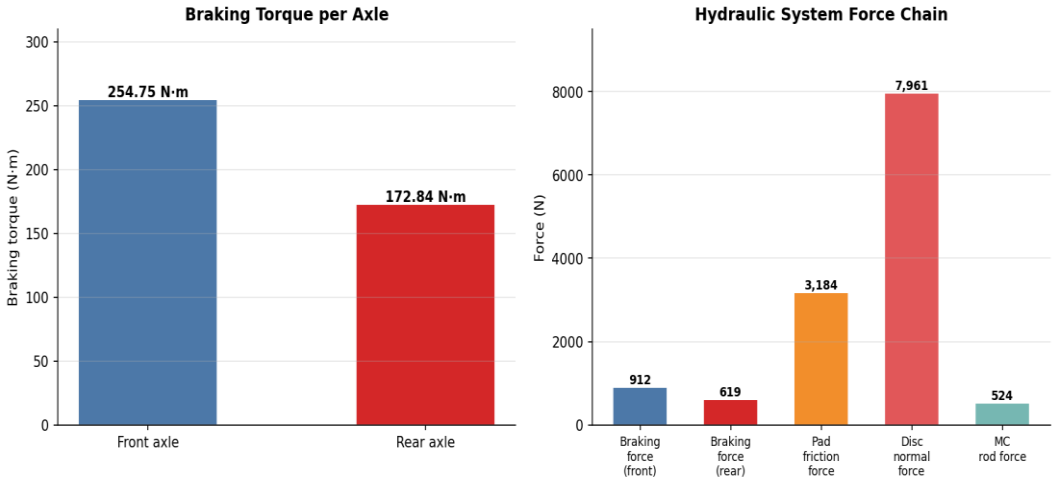
Source: Authors, 2026.

The front axle concentrates 59,6% of the total braking force (Ffd = 912 N) and the rear axle 40,4% (Fft = 619 N), justifying the adoption of Ø160 mm (254,75 N·m) and Ø140 mm (172,84 N·m) discs. As illustrated in Figure 4, the mechanical-hydraulic chain amplifies 87,29 N at the pedal to 524 N at the master cylinder (6:1 ratio and area ratio), generating a pressure of ~1,75 MPa and a friction force of ~3.184 N on the brake pads. The estimated stopping distance is 10,58 m from 40 km/h (μ = 0,60).

REMUNOM
ISSN 2178-6925

Received: 13/03/2026 - **Accepted:** 20/05/2026
Vol: 13.10
DOI: 10.66104/fn0sgw57
Pages: 1-27

Figure 3: Required braking torques per axle and hydraulic force amplification chain



Source: Authors, 2026.

.

All analytical results obtained in the brake system design are consolidated in Table 6, including static and dynamic reactions, brake force distribution, axle torques, friction forces on the pads, normal force on the disc, hydraulic pressure, forces on the master cylinder and pedal, as well as the estimated stopping distance.

Table 6: Analytical sizing results for the braking system.

Quantity	Symbol / Eq.	Result
Static reaction – rear axle	Fet (Eq. 1)	1.700,00 N
Static reaction – front axle	Fed (Eq. 1)	850,20 N
Dynamic reaction – front (a = 0,60 g)	Fn,f (Eq. 2)	1.519,61 N (+78,6%)
Dynamic reaction – rear (a = 0,60 g)	Fn,r (Eq. 2)	1.030,99 N (−39,4%)
Braking force – front axle	Ffd (Eq. 3)	912,00 N (59,6%)
Braking force – rear axle	Fft (Eq. 3)	619,00 N (40,4%)
Braking torque – front	Tn,f (Eq. 4)	254,75 N·m
Braking torque – rear	Tn,r (Eq. 4)	172,84 N·m
Pad friction force – front	Fat,f (Eq. 5)	3.184,40 N
Pad friction force – rear	Fat,r (Eq. 5)	2.160,50 N
Disc normal force – front	Fn,disc (Eq. 6)	7.961,00 N
Hydraulic pressure	P (Eq. 7)	1,75 MPa
Master cylinder rod force	Fhc (Eq. 8)	524,00 N

REMUNOM
ISSN 2178-6925

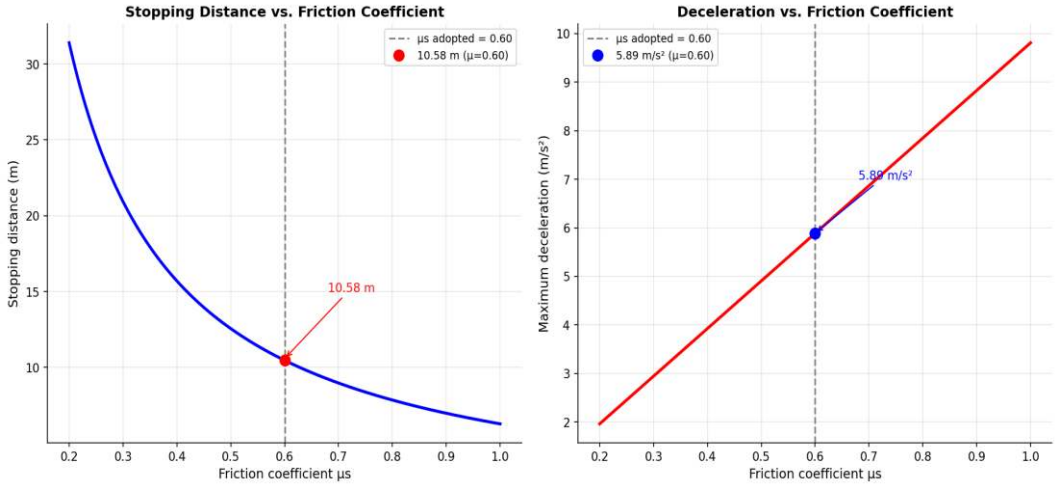
Received: 13/03/2026 - **Accepted:** 20/05/2026
Vol: 13.10
DOI: 10.66104/fn0sgw57
Pages: 1-27

Pedal effort	Fpedal (Eq. 9)	87,29 N
Pedal safety factor	FS	2,46
Stopping distance	d (Eq. 10)	10,58 m

Source: Authors, 2026.

The curves were generated by the relationships a = μs•g and d = v_0^2/(2•μs•g), with v_0 = 11,1 m/s. Figure 5 shows the relationship between the tire-ground friction coefficient (μ), the maximum deceleration, and the stopping distance. It can be observed that the deceleration varies linearly with μ, as predicted by the dynamic model, while the stopping distance decreases non-linearly, indicating greater sensitivity of the system in low-adhesion conditions. This behavior has direct design implications, since, in off-road environments, small variations in μ can result in significant increases in stopping distance, justifying the adoption of conservative criteria. The nominal point (μ=0,60) places the system in an efficient operating range, in accordance with the literature for light off-road vehicles (El-Gindy; El-Sayegh, 2023).

Figure 5: Stopping distance and maximum deceleration as a function of tyre–ground friction coefficient.



Source: Authors, 2026

4.2. Braking Efficiency and Ideal Cornering

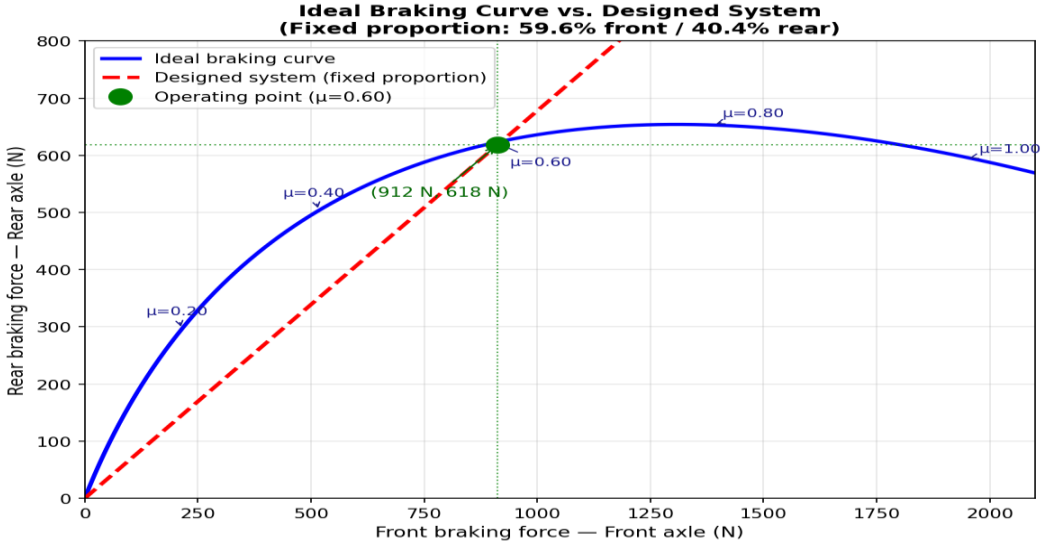
Figure 6 shows that the fixed braking distribution (59.6% front / 40.4% rear) closely matches the ideal braking curve up to μ ≈ 0.60, where the system reaches near-optimal grip utilization (η > 90%), validating the consistency between the

REMUNOM
ISSN 2178-6925

Received: 13/03/2026 - **Accepted:** 20/05/2026
Vol: 13.10
DOI: 10.66104/fn0sgw57
Pages: 1-27

longitudinal dynamics model and the hydraulic design. However, for μ > 0.70, a progressive deviation occurs, with increased rear axle braking force and a tendency for premature rear wheel lock, highlighting a typical limitation of fixed-ratio systems that can be mitigated with proportional brake valves.

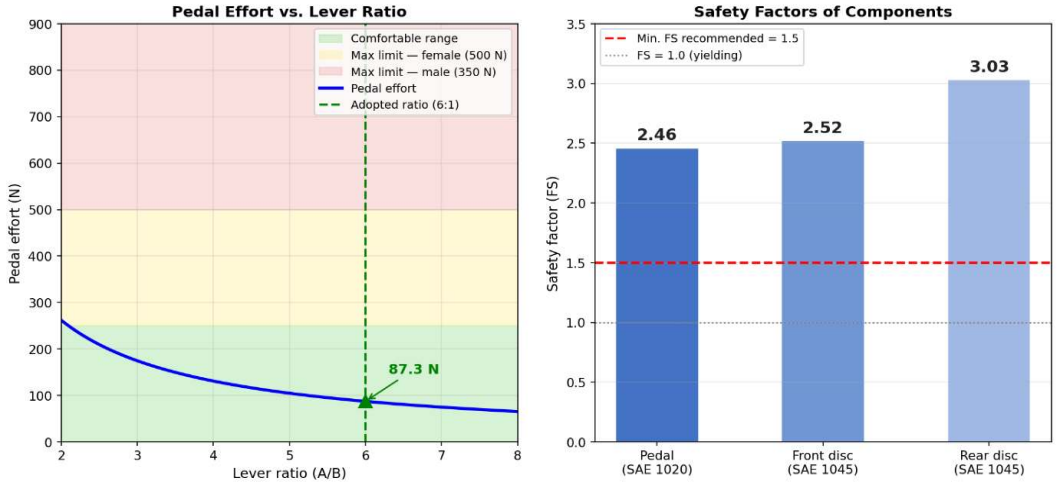
Figure 6: Ideal braking curve and real force distribution of the projected system (fixed ratio 59,6%/40,4%)



Source: Authors, 2026

Figure 7 shows the brake pedal effort as a function of the lever ratio, with ergonomic reference bands, and the structural safety factors of the system components.

Figure 7: (Left) Brake pedal effort as a function of the lever ratio, with ergonomic reference bands according to Budynas and Nisbett (2020); (Right) Structural safety factors obtained in the FEA analyses for the pedal (FS = 2,46), front disc (FS = 2,52), and rear disc (FS = 3,03).



Source: Authors, 2026

REMUNOM
ISSN 2178-6925

Received: 13/03/2026 - **Accepted:** 20/05/2026
Vol: 13.10
DOI: 10.66104/fn0sgw57
Pages: 1-27

The effort of 87,29 N on the pedal is within the ergonomic limits established in the literature (100–500 N). Structurally, the pedal (SAE 1020) has FS = 2,46 and tension distribution without critical concentrations, while the front and rear discs have FS = 2,52 and 3,03, respectively. All components operate in an elastic regime with adequate margins for dynamic stresses typical of off-road applications.

4.3. Structural FEA Results

The results of the static structural analyses of the braking system components are consolidated in Table 7.

Table 7- Summary of static structural FEA results for braking system components.

Component	Material	Sy (MPa)	σvM,max (MPa)	FS	Regime
Brake pedal	SAE 1020	350	142,35	2,46	Elastic
Front disc (Ø160 mm)	SAE 1045	530	~210*	2,52	Elastic
Rear disc (Ø140 mm)	SAE 1045	530	~175*	3,03	Elastic

Source: Authors, 2026

Table 7 consolidates the structural results of three components: the pedal (SAE 1020) recorded σvM,max = 142,35 MPa with FS = 2,46; the front disc (SAE 1045, Ø160 mm) reached σvM,max ≈ 210 MPa with FS = 2,52; the rear disc (Ø140 mm) recorded σvM,max ≈ 175 MPa with FS = 3,03, both discs under conservative loading of 6.384 N. All components operate in an elastic regime, with stresses lower than the respective yield limits. The von Mises stress distribution on the pedal is presented in Figure 8, evidencing concentration in the chassis joint region.

REMUNOM
ISSN 2178-6925

Received: 13/03/2026 - **Accepted:** 20/05/2026
Vol: 13.10
DOI: 10.66104/fn0sgw57
Pages: 1-27

Figure 8: Von Mises equivalent stress distribution on the brake pedal (SAE 1020) — ANSYS Workbench.



Source: Authors, 2026

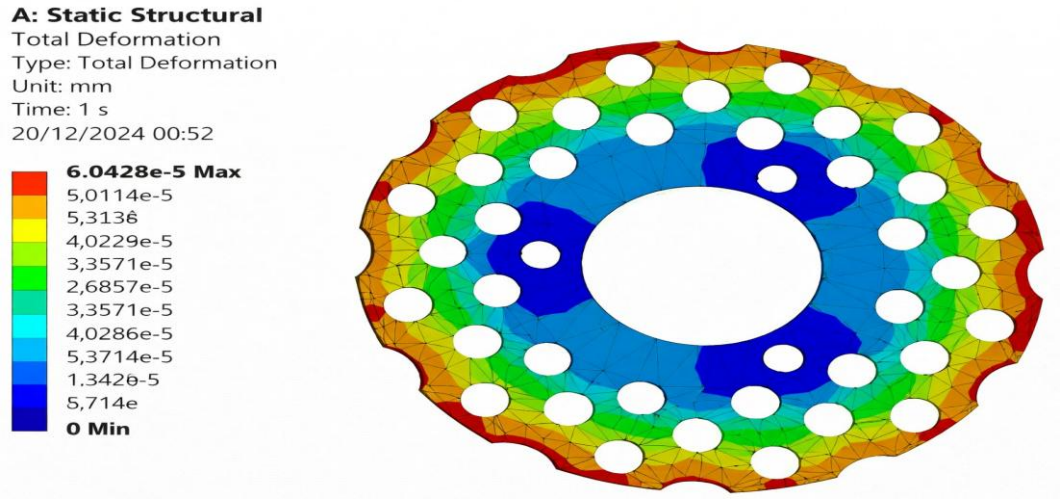
Finite element structural analysis of the brake pedal, manufactured from SAE 1020 steel, revealed a maximum von Mises stress of 142.35 MPa, concentrated in the critical region of fixation to the chassis, where stress intensification is expected due to geometric constraints and load transmission. When compared to the material's yield strength (350 MPa), this results in a safety factor of FS = 2.46, indicating a robust structural margin. The stress distribution confirms that the component operates entirely within the elastic regime, with no indication of plastic deformation under the applied loading conditions. Additionally, this safety factor exceeds the minimum design criterion of FS ≥ 1.5 typically adopted for components subjected to cyclic loading, reinforcing the reliability and durability of the design under repeated service conditions.

Complementarily, Figure 9 illustrates the total deformation distribution of the brake disc, manufactured in SAE 1045 steel, as obtained through simulation in ANSYS Workbench. The results provide insight into the displacement field and structural behavior of the disc under braking loads, supporting the overall validation of the braking system from a structural standpoint.

REMUNOM
ISSN 2178-6925

Received: 13/03/2026 - **Accepted:** 20/05/2026
Vol: 13.10
DOI: 10.66104/fn0sgw57
Pages: 1-27

Figure 9: Total deformation distribution on the front brake disc (SAE 1045, Ø160 mm) — ANSYS Workbench.



Source: Authors, 2026

The discs in SAE 1045 have a maximum total deformation of 6,04 × 10^{-5} mm in the peripheral region and reduced deformations in the hub, in accordance with the expected loading profile.

This deformation gradient, maximum in the periphery and minimum in the hub, is consistent with the compressive load pattern located in the pad-disc contact zone, corroborating the results reported by Reghunath et al. (2021) and Oladeji et al. (2022). The safety factors of 2,52 (front disc) and 3,03 (rear disc) show a wide structural margin, confirming the mechanical integrity of the brake system.

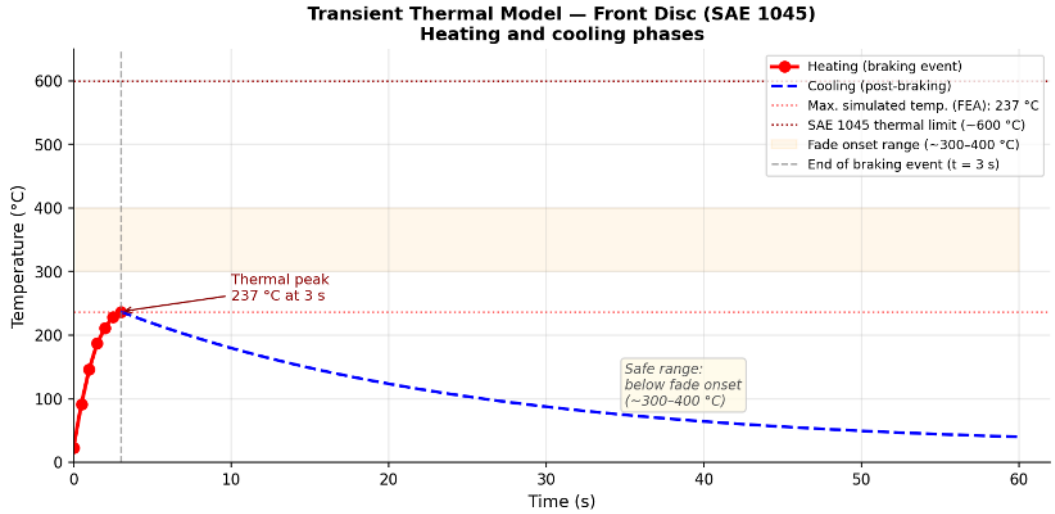
4.4. Transient Thermal Analysis

Figure 10 presents the temporal evolution of the maximum and minimum temperatures of the front brake disc during the 3 s braking event, as obtained through transient finite element analysis (FEA). The results capture the rapid thermal response of the component under frictional heating, highlighting the temperature gradients established between the contact region (disc–pad interface) and the remaining volume of the disc. This transient behavior is essential for evaluating thermal stability, potential hot spots, and the influence of heat accumulation on braking performance and material integrity over short-duration, high-energy braking cycles.

REMUNOM
ISSN 2178-6925

Received: 13/03/2026 - **Accepted:** 20/05/2026
Vol: 13.10
DOI: 10.66104/fn0sgw57
Pages: 1-27

Figure 10: Temporal evolution of the maximum and minimum temperature of the front disc (SAE 1045, Ø160 mm) during the 3 s braking event, obtained by transient FEA in ANSYS Workbench 2024.

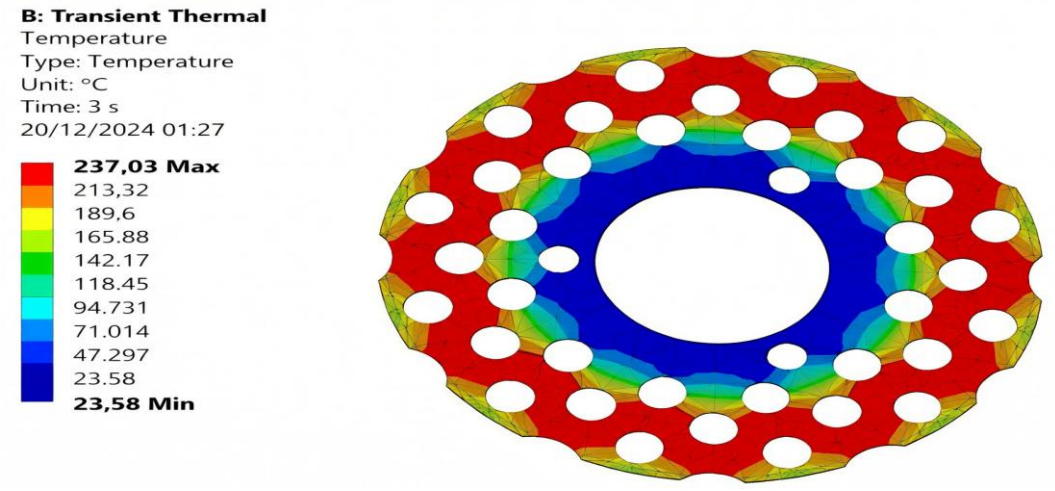


Source: Authors, 2026

The maximum temperature of 237,03 °C is concentrated in the annular region of the pad-disc contact, while the hub region remains close to the initial temperature (23,58 °C), confirming the pronounced radial thermal gradient expected for this type of component (Belhocine; Abdullah, 2020).

The spatial distribution of the gradient can be observed in the temperature map at t = 3 s shown in Figure 11.

Figure 11: Transient temperature field on the front brake disc (SAE 1045, Ø160 mm) at t = 3 s – ANSYS Workbench 2024.



Source: Authors, 2026

The map shows the confinement of heat in the friction zone and the effectiveness of radial thermal dissipation in the remaining segments of the disc.

REMUNOM
ISSN 2178-6925

Received: 13/03/2026 - **Accepted:** 20/05/2026
Vol: 13.10
DOI: 10.66104/fn0sgw57
Pages: 1-27

The results of the transient thermal analysis of the front disc are summarized in Table 8.

Table 8: Transient thermal analysis results - front disc (SAE 1045, Ø160 mm)

Parameter	Value	Observation
Maximum temperature – FEA (t = 3 s)	237,03 °C	Pad–disc contact region
Minimum disc temperature	23,58 °C	Hub region
Thermal operating limit – SAE 1045	~600 °C	Ashby; Jones (2012)
Thermal margin to limit	~60,5%	Relative to material limit
Cooling time (to Tamb + 10 °C)	~27 s	Lumped capacitance (h = 80 W/m²K)
Biot number	Bi < 0,1	Validity criterion: Yin et al. (2023)

Source: Authors, 2026

A maximum temperature of 237.03 °C corresponds to approximately 39.5% of the operational limit of SAE 1045 (~600 °C), resulting in a thermal margin of 363 °C (60.5% of the allowable range remaining), according to Ashby and Jones (2012). This indicates that the disc operates well below critical temperature thresholds, ensuring a significant safety margin against thermal degradation mechanisms, particularly brake fade associated with reduced friction coefficient and material softening at elevated temperatures. Furthermore, the predicted temperature level suggests that no substantial microstructural transformations or loss of mechanical strength are expected under the analyzed braking condition.

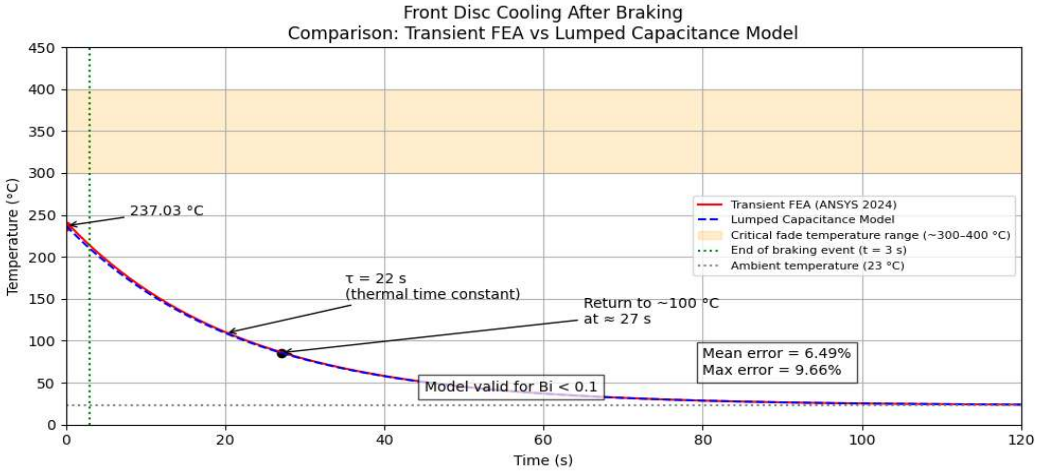
This result is consistent with the findings of Oladeji et al. (2022), who reported maximum temperatures in the range of 200–240 °C for solid carbon steel discs under short-duration, single braking events. It also aligns with the coupled thermomechanical simulations presented by Yin et al. (2023), reinforcing the validity of the adopted transient thermal model and its assumptions regarding heat generation, distribution, and dissipation during braking.

Figure 12 compares the cooling curve obtained by transient FEA with the analytical estimate of the concentrated capacitance model. The analytical curve is described by $T(t) = T_amb + (T_0 - T_amb) \cdot \exp(-t/\tau)$, with $\tau = \rho \cdot V \cdot cp/(h \cdot A)$, $T_0 = 237{,}03$ °C and $h = 80$ W/m²K.

REMUNOM
ISSN 2178-6925

Received: 13/03/2026 - **Accepted:** 20/05/2026
Vol: 13.10
DOI: 10.66104/fn0sgw57
Pages: 1-27

Figure 12: Cooling curve of the front disc after a braking event (T_0 = 237,03 °C): comparison between transient FEA (ANSYS Workbench 2024) and the analytical model of concentrated capacitance.



Source: Authors, 2026

The agreement between the two models, with an average deviation of less than 7%, confirms the applicability and reliability of the simplified thermal approach for the analyzed geometry and convection conditions, particularly considering that the Biot criterion (Bi < 0.1) is satisfied. This indicates that the lumped capacitance assumption is valid, with negligible internal temperature gradients relative to surface heat transfer, thereby justifying the use of a reduced-order model without significant loss of accuracy.

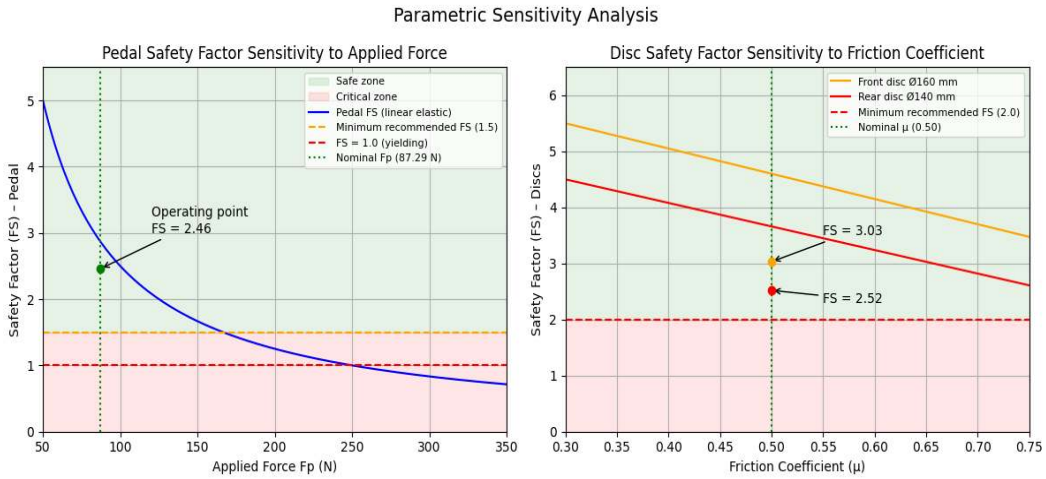
From an operational standpoint, the disc cools down to approximately ~100 °C within about 27 seconds after the braking event, characterizing a thermal recovery time compatible with the typical intervals between braking cycles in Baja SAE competitions. This relatively fast heat dissipation suggests efficient convective and conductive heat transfer mechanisms, preventing excessive thermal accumulation. Consequently, the system demonstrates low susceptibility to thermal saturation under repeated braking, which is a critical factor in maintaining consistent friction performance.

Furthermore, this behavior reduces the likelihood of progressive brake fade caused by successive thermal cycles, preserving both the friction coefficient stability and the structural integrity of the disc over time. These findings reinforce the robustness of the thermal design under realistic operating conditions. Figure 13 presents a parametric sensitivity analysis of two safety factors, providing additional insight into the influence of key design variables on system performance and reliability.

REMUNOM
ISSN 2178-6925

Received: 13/03/2026 - **Accepted:** 20/05/2026
Vol: 13.10
DOI: 10.66104/fn0sgw57
Pages: 1-27

Figure 13: Parametric sensitivity analysis of the safety factors: (Left) variation of the pedal safety factor as a function of the applied pedal force; (Right) variation of the disc safety factors as a function of the pad-disc friction coefficient (μp).



Source: Authors, 2026

In the graph on the left, it is observed that the safety factor of the pedal decreases inversely proportional to the applied force, maintaining the minimum limit of FS ≥ 1,5 even for forces close to the maximum ergonomic limit of 500 N, which confirms the structural robustness of the component in all operational aspects. In the right graph, the safety factors of the discs show a progressive reduction with the increase of the pad–disc friction coefficient μp, expected behavior given that higher values of μp directly increase the normal force required on the disc. Likewise, both discs maintain FS above 2,0 even for μp = 0,70, evidencing an adequate structural margin against variations in the tribological properties of the pads over the long useful life of the system. These results reinforce that the project is robust not only for the nominal operating conditions, but also for realistic parametric deviations.

4.5. Limitations of the Model and Operational Premises

The interpretation of the results must consider the premises adopted in the model, which delimit the conclusions. (i) Constant friction coefficients: the values of μs and μp are treated as fixed parameters throughout the braking event, without considering variations in temperature, slippage or contamination by mud and water — typical off-road operating conditions. (ii) Simplified convection: the coefficient h = 80

REMUNOM
ISSN 2178-6925

Received: 13/03/2026 - **Accepted:** 20/05/2026
Vol: 13.10
DOI: 10.66104/fn0sgw57
Pages: 1-27

W/m²K was assumed uniform over the entire disc surface, without modelling airflow. (iii) Absence of repeated braking cycles: the model simulates a single 3 s event; heat accumulation in repeated cycles and thermal fatigue are not evaluated. (iv) Absence of structural fatigue: the analysis is static; disc ovalization, warping, and wear under prolonged service are not modelled. (v) Absence of experimental testing: all results are only numerical and analytical; Experimental validation with a physical prototype constitutes an essential stage before manufacturing. (vi) Idealized longitudinal model: vehicle dynamics exclusively consider longitudinal load transfer on a flat and homogeneous surface, not representing the full spectrum of off-road operation.

5. Conclusion

This work demonstrates the technical feasibility of a disc brake system for small off-road vehicles through integrated computational verification methodology, combining analytical modeling, hydromechanical dimensioning and finite element simulation. The dynamic analysis of load transfer is based on the adopted asymmetrical configuration, in that the dimensioning is intended to ensure the effort of actuation compatible with the ergonomic limits and braking efficiency adequate to the approved operating conditions. The structural simulations confirm the mechanical integrity of the components in an elastic regime, with satisfactory safety factors, and the thermal analysis shows that the maximum temperatures remain below two critical fade limits, with cooling behavior consistent with the reference analytical models.

The agreement between the numerical and analytical results confirms the robustness of the proposed approach and its potential as a systematic tool for the development and optimization of braking systems in competitive applications. The limitations of the model, detailed in Section 4.5, delimit the scope of the conclusions: the friction coefficients were treated as constants, the convection was simplified, cyclic brakes and fatigue were not validated, and the dynamic model represents an idealized longitudinal condition. These premises are adequate for the conceptual project phase, but must be relaxed in subsequent experimental verification. As future perspectives, we highlight the experimental validation of the models under cyclic thermal regimes, the fatigue analysis of the discs and the incorporation of active control strategies for

REMUNOM
ISSN 2178-6925

Received: 13/03/2026 - **Accepted:** 20/05/2026
Vol: 13.10
DOI: 10.66104/fn0sgw57
Pages: 1-27

the distribution of braking forces.

Acknowledgments

The authors are grateful to the Instituto Federal de Educação, Ciência e Tecnologia da Paraíba (IFPB), Campus Cajazeiras, for institutional support, to the Laboratório Cajazeirense de Processos de Produção- LC2P and for the availability of the infrastructure necessary for the development of this work.

References

ASHBY, M. F.; JONES, D. R. H. **Engineering Materials 1: An Introduction to Properties, Applications and Design**. 4. ed. Oxford: Elsevier Butterworth-Heinemann, 2012.

BELHOCINE, A.; ABDULLAH, O. I. A thermomechanical model for the analysis of disc brake using the finite element method in frictional contact. **Journal of Thermal Stresses**, v. 43, n. 3, p. 305–320, 2020. Disponível em: https://doi.org/10.1080/01495739.2019.1683482

BUDYNAS, R. G.; NISBETT, J. K. **Shigley's Mechanical Engineering Design**. 11. ed. New York: McGraw-Hill Education, 2020.

CHATURVEDI, K. et al. Comparative study on thermal analysis of disc brake using ANSYS simulation. AIP **Conference Proceedings**, v. 2869, p. 040015, 2023. Disponível em: https://doi.org/10.1063/5.0163541

EL-GINDY, M.; EL-SAYEGH, Z. **Road and Off-Road Vehicle Dynamics**. Cham: Springer Nature, 2023. Disponível em: https://doi.org/10.1007/978-3-031-36216-3

GERDAU. **Propriedades Mecânicas dos Aços SAE 1020 e SAE 1045**. [Catálogo técnico]. Brasil: Gerdau S.A., 2020. Disponível em: https://www2.gerdau.com.br/sites/Tabela_Composicao_Quimica. Acesso em: 10 jan. 2026.

NOOHI, F.; NIKOOBIN, A.; ASHORY, M. R. Developing an accurate finite element model for brake disc in contact with the pad using experimental modal analysis. **Proceedings of the** Institution **of Mechanical Engineers**, Part D: Journal of Automobile Engineering, 2024. Disponível em:

REMUNOM
ISSN 2178-6925

Received: 13/03/2026 - **Accepted:** 20/05/2026
Vol: 13.10
DOI: 10.66104/fn0sgw57
Pages: 1-27

https://doi.org/10.1177/09544070241295411. Acesso em: 13 jan. 2026. Publicação antecipada online.

OLADEJI, J. A. et al. Thermo-mechanical behavior of aluminum matrix nano-composite automobile disc brake rotor using finite element method. **Applied Sciences**, v. 12, n. 18, p. 9057, 2022. Disponível em: https://doi.org/10.3390/app12189057

PRAKASH, C.; PRAKASH, J. Investigation and selection of optimistic material for two wheeler brake disc: an experimental and finite element approach. **Proceedings of the Institution of** Mechanical **Engineers**, Part D: Journal of Automobile Engineering, 2024. Disponível em: https://doi.org/10.1177/09544070241254148. Acesso em: 13 jan. 2026. Publicação antecipada online.

REGHUNATH, R. et al. Design and analysis of brake disc assembly for an FSAE vehicle. **Materials Today: Proceedings**, v. 47, p. 4491–4500, 2021. Disponível em: https://doi.org/10.1016/j.matpr.2021.05.255

SAE BRASIL. **Regulamento** Baja **SAE Brasil 2024**. São Paulo: SAE Brasil, 2024.

SAVIO, D. et al. Influence of road profiles and truck braking on the dynamic load transfer to the pavement. International **Journal of Pavement Engineering**, v. 24, n. 2, 2022. Disponível em: https://doi.org/10.1080/10298436.2022.2090559

TUNG, N. T.; VAN VAN, L. Studying the efficiency of car brake force distribution by a three-dimensional dynamics model. In: NGUYEN-XUAN, H. et al. (ed.). **Proceedings of the 3rd Annual International Conference on Material, Machines and Methods for Sustainable Development (MMMS2022)**. . Cham: Springer Nature, 2023. p. 281–290. Disponível em: https://doi.org/10.1007/978-3-031-31824-5_29. Acesso em: 13 jan. 2026.

YIN, X. et al. Thermal stress simulation and fatigue life of commercial vehicle disk brakes under emergency braking conditions. **AIP Advances**, v. 13, n. 12, p. 125220, 2023. Disponível em: https://doi.org/10.1063/5.0164109